80-10083
TM-80582

NASA

Technical Memorandum 80582

Multisensor Analysis of Hydrologic Features in the Wind River Range, Wyoming with Emphasis on the Seasat SAR

(E80-10083) MULTISENSOR ANALYSIS OF HYDROLOGIC FEATURES IN THE WIND RIVER RANGE, WYOMING WITH EMPHASIS ON THE SEASAT SAR (NASA) 26 p HC A03/MF A01 CSCL 08H N80-19591
Unclas
G3/43 00083

James L. Foster and Dorothy K. Hall

Original photography may be purchased from:
EROS Data Center

Sioux Falls, SD 57198

OCTOBER 1979

National Aeronautics and
Space Administration

Goddard Space Flight Center
Greenbelt, Maryland 20771

MULTISENSOR ANALYSIS OF HYDROLOGIC FEATURES IN THE WIND RIVER RANGE, WYOMING WITH EMPHASIS ON THE SEASAT SAR

James L. Foster

Dorothy K. Hall

ABSTRACT

Synthetic Aperture Radar (SAR) imagery of the Wind River Range area in Wyoming is compared to visible and near-infrared imagery of the same area. Data from the Seasat L-Band SAR and an aircraft X-Band SAR are compared to Landsat Return Beam Vidicon (RBV) visible data and near-infrared aerial photography and topographic maps of the same area. Visible and near-infrared data provide more information than the SAR data when conditions are optimum. However, the SAR penetrates clouds and snow, and data can be acquired day or night. Drainage density detail is good on SAR imagery because individual streams show up well due to riparian vegetation causing higher radar reflections which result from the "rough" surface which vegetation creates. In the winter image, the X-Band radar data show high returns resulting from cracks on the lake ice surfaces. High returns are also evident in the L-Band SAR imagery of the lakes due to ripples on the lake surfaces induced by wind. It is concluded that utilization of multispectral data (visible, near-infrared and microwave (radar)) would optimize analysis of hydrologic features.

CONTENTS

MULTISENSOR ANALYSIS OF HYDROLOGIC FEATURES IN THE WIND RIVER RANGE, WYOMING WITH EMPHASIS ON THE SEASAT SAR

I. INTRODUCTION

In this paper, a multispectral approach was employed for analysis of hydrologic features in the Wind River Range, Wyoming. Emphasis is placed on the Seasat Synthetic Aperture Radar (SAR) because it provides a new data source. The intent of this study was to assess the information content of the Seasat SAR by comparing the L-Band (23.5 cm wavelength) Seasat SAR data with X-Band (3.1 cm) aircraft SAR data, Landsat-3 return beam vidicon (RBV) data, U-2 color-infrared photography and topographic maps. The capabilities of the Seasat SAR for hydrologic studies in the Wind River Range area could truly be assessed because data from several different sensors were available for comparison. For this reason, the Wind River Range was chosen for study. Seasat SAR data provided minimal improvements as compared to other sensors for studying hydrologic features in this study area. These improvements resulted from the day/night, all-weather capabilities of the Seasat SAR. Imagery was acquired on the following dates: Seasat SAR - July 31, 1978, aircraft SAR - March 30, 1979, Landsat-3 RBV - August 11, 1978, U-2 photography - March 21, 1976 and June 21, 1976. No ground truth data were available for comparison with the remotely-sensed data. Other work dealing with active microwave applications to hydrology has been performed. For example, soil wetness and snowmelt measurements were cited by Simonett (1978) as two important areas for which radar data could be useful for water resources studies.

II. STUDY AREA

The Wind River Mountain Range is located in west-central Wyoming (Figures 1A and B). Precambrian metamorphic and plutonic rocks and limestone, sandstone and granitic lithologies comprise the geology of the area. The climate varies with altitude, being semi-arid at the base of the range at approximately 1830 m (6000 feet), and alpine at the summits at an elevation of nearly 4265 m (14,000 feet). Precipitation averages 300 mm (12 inches) a year at the base and over 1525 mm (60 inches) on the highest peaks. Approximately two-thirds of this precipitation runs off via

streamflow. As a result of the climate, latitude and topography there are 63 small valley glaciers in the Wind River Range many of which are advancing.

The vegetation in the Wind River Range consists of alpine meadows and herbaceous plants above 3050 m (10,000 feet); below this Douglas Fir is common near the base of the mountains, and Lodgepole Pine and Western Spruce-Fir forests dominate the higher slopes. Sagebrush, wheatgrass and steppe vegetation can be found near the base of the mountains. In addition, cottonwood and willow trees are prevalent on the floodplains of many of the larger streams near the base of the mountains.

III. SENSORS

L-BAND SAR (SEASAT)

The Seasat satellite was placed in a circular near-polar orbit in June of 1978. Seasat circled the Earth 14 times per day completing 1503 revolutions prior to a power failure which terminated all remote-sensing capabilities in October of 1978. Synthetic aperture radar (SAR) imagery was acquired for brief periods when the satellite was in direct line-of-sight communication with one of the four receiving stations in North America or the receiving station in the United Kingdom. SAR imagery was acquired over most of the U.S., but total coverage of the continental land surfaces was not obtained.

A photograph is a record of the intensity of light reflected from each resolution cell within a camera's field-of-view, whereas a radar image is a record of the intensity of microwave energy reflected from each resolution cell within the radar field-of-view. Like conventional radar, the SAR transmits electromagnetic pulses and records their return, or echo (Kovaly, 1978). The Seasat SAR antenna transmissions are spread over an angle of slightly less than 1.5°, which means that a given spot on the Earth's surface is within the beam for 2 seconds since SAR is moving along its orbit about 7.4 km/sec. Return echoes from this beam are integrated over that 2 second period so that each ground spot returns the radar beam from a range of angles. The synthetic aperture is a product of the orbital velocity of the satellite and the integration time. This results in an image having higher clarity and better resolution than imagery from real aperture systems operating at the

same altitude. In addition, the resolution of the imagery is independent of altitude. The Seasat SAR can resolve details as small as 25 m. The actual resolution is better than 7 m, but to reduce scattering effects called "speckle" in the return signal, four resolution units are averaged together, reducing the resolution of the finished product nearly four times. The scale of the SAR imagery is approximately 1:450,000.

Radar has its own source of illumination and is therefore not restricted to daytime operation. Microwave signals at the Seasat SAR wavelength are usually unaffected by clouds, fog and atmospheric disturbances resulting in an all weather measurement capability. Seasat SAR data result from horizontally like-polarized (HH) L-band (23.5 cm) radar signals taken during ascending or descending orbital modes. The intensity or brightness of an individual resolution cell is related to backscatter energy from the source. More scattering will cause a brighter return. The surface parameters which have been found to affect the return signal are surface roughness, slope and the complex dielectric constant (MacDonald and Waite, 1973). Incidence angle, polarization and frequency are the instrument parameters which also affect the intensity or brightness of the return signal.

Relative surface roughness is calculated by using the smooth and rough criteria of Peake and Oliver (1971). These criteria are:

smooth criterion	rough criterion
$h < \frac{\lambda}{8 \sin \gamma}$	$h > \frac{\lambda}{4.4 \sin \gamma}$

where h = the average height of surface irregularities

λ = the radar wavelength (23.5 cm for Seasat SAR)

γ = the depression angle between the horizontal plane and the radar wave incident upon the terrain (70° for Seasat SAR)

For the Seasat SAR the smooth criterion is calculated to be 3.1 cm which means that surfaces with a vertical relief of 3.1 cm or less within the SAR footprint (25 m) will appear smooth and have a dark signature. The rough criterion is 5.7 cm which means that surfaces with a vertical relief of 5.7 cm or more will appear rough and have a bright signature. Surfaces with vertical relief between 3.1 and 5.7 cm will have intermediate signatures (Sabins et al., 1979).

The dynamic range of the Seasat SAR system is low, corresponding to a maximum of 6 gray levels. For this reason the more subtle variations in surface conditions are sometimes not seen. The Seasat SAR has a look angle of about 20° (the depression angle is about 70°) and incidence angles that commonly range between 0° and 30°. Surfaces normal to the radar look direction having a slope angle larger than 20° may yield incidence angles of 0° and will be geometrically distorted due to the layover effect whereby foreslopes appear foreshortened because the radar echo is returned to the source sooner than echos from other slopes (Matthews, 1975). Because of the scale of the Seasat imagery and the narrow radar beam width (6°), image distortion is not a serious problem. The corollary to layover of foreslopes is shadowing of backslopes which occurs where the slopes are steeper than the depression angle (70°). In this study area most slopes do not approach 70°, consequently most backslopes are not in radar shadow (Ford, 1979).

X-BAND SAR (AIRCRAFT)

The X-Band system used in this study is a synthetic aperture radar and is flown on-board the NASA RB-57 aircraft, typically at an altitude of 2088 m (60,000 feet). This SAR images a swath of ~16.1 km (10 miles) on the ground. The instrument operates at a wavelength of ~3.1 cm (9600 ± 5 KHz) with a range and azimuth resolution of ~15.2 m (50 feet). Like (HH and VV) and cross-polarized (HV and VH) data are taken simultaneously. Data can be obtained in two modes. In mode I, the viewing angle (off-nadir) can be set between 14° and 51°. In mode II, the viewing angle can be set for any angle between 45° and 63° off-nadir. Viewing angles can be selected in the cockpit.

Comparison of the HH and VV with the HV and VH images of the same area show that the radar return signals are generally higher in the like-polarized imagery as seen in Figure 3. Mode I imagery gave higher returns than Mode II data, so only Mode I imagery is included in this analysis. Some banding is present in the imagery and hinders interpretation where it occurs.

The rough criterion for the X-Band SAR is calculated to be 1.1 cm, and the smooth criterion is 0.6 cm using the depression angle of 38.7°. The X-Band SAR depression angle is considerably less than that of the Seasat SAR (70°), and thus radar shadowing of backslopes is created in the resulting X-Band imagery.

U-2 CAMERA

Aerial photography was taken over the Wind River Range as part of the NASA Earth Resources Aircraft Program (ERAP) from 1974 through 1976. Using an RC-8 camera on-board a U-2 aircraft, approximately 10 meter resolution imagery was obtained in the 0.5 μm - 1.1 μm spectral range. The U-2 aircraft photographs the Earth from an altitude of about 18,300 m (60,000 feet), with a focal length of 15 cm (6 inches). The scale of this high altitude photography is approximately 1:120,000.

LANDSAT RBV

Landsat imagery has been acquired over the Wind River Range since July of 1972 when Landsat-1 was first launched. Landsat-2 was launched in January of 1975 and Landsat-3 in March of 1978. The Landsat satellites have high resolution multispectral sensors, repetitive coverage capability and cartographic fidelity. In addition to the multispectral scanner subsystem (MSS) on-board all three Landsat satellites, Landsat-3 also has a Return Beam Vidicon (RBV) system which employs two panchromatic vidicon cameras that operate in the 0.51-0.75μm band. The RBV imagery has a nominal resolution of ~30 m and a scale of 1:500,000. Four overlapping Landsat-3 RBV subscenes comprise one MSS scene.

IV. ANALYSIS AND RESULTS

The Seasat SAR image (Figure 2) was taken on July 31, 1978 in a descending orbital mode (NE to SW). For this orbit the look direction is towards the NW. This scene shows the Wind River, Gros Ventre and Wyoming Ranges of Wyoming and the Wyoming Basin. The bright or high return areas represent a high surface roughness within the SAR footprint (25 m). Dark or low return areas represent smooth surfaces. The bright returns in the mountains are largely a result of the forest canopy covering the mountain slopes (for example, see area A on Figare 2). Forested areas have a high surface roughness. The forest canopy conceals the underlying surface by reflecting away radar energy.

Faults and lineaments within the mountainous areas can be easily detected on the SAR image as abrupt gray level changes as seen at "B" on Figure 2. Mountain slopes which face the look

direction of the SAR reflect radar energy back to the antenna and produce brighter signatures than slopes facing away which appear darker.

The Wyoming Basin appears dark in the center of the image as seen in Figure 2 marked "C". The relatively smooth terrain gives a low radar return and as a result, rivers and streams within this low return region show up as high return or bright features because of the vegetation confined to stream banks and floodplains having a high surface roughness relative to the non-vegetated surrounding plains (Sabins et al, 1979). This can be seen in area "D" on Figure 2.

At the base of the Wind River Mountains, north of the New Fork River, several glacial lakes are visible on the Seasat image. The lakes vary in brightness from black to gray. Ripples and waves on the lake surfaces most likely produce higher returns and smooth, calm water produces lower returns (Sabins et al., 1979). The lakes (areas marked "E" on Figure 2) will be discussed in more detail later.

The bright streaks in the lower right corner of the image (area F) are perhaps associated with precipitating clouds. Precipitation was recorded at several locations in west-central Wyoming on the day of the Seasat overpass, and the Geostationary Operational Environment Satellite (GOES) confirmed the presence of cumulonimbus cloud cells south of the Wind River Range at the same hour that the Seasat image was taken (9:00 P.M. local time). Landsat imagery, U-2 photography and topographic and geologic maps of the same area do not indicate the presence of any surface features which could otherwise explain these returns. It is also possible that these returns may be caused by differences in soil moisture resulting from precipitation which occurred earlier in the day.

The area of bright returns in the lower right hand center of the image (area "G") is non-vegetated but the rough (highly dissected) surface results in a high reflectivity of the radar energy. A marsh area transitional in brightness between the vegetated stream channels and the dark basin areas can be seen at area "H" on Figure 2.

Dendritic drainage characterizes this part of Wyoming. The combination of high surface runoff and non-resistant and impermeable bedrock results in a highly dissected surface. The associated

drainage features give high returns and thus appear bright on the radar imagery. The effect of radar layover, discussed earlier, tends to enhance small valleys which dissect ridges and slopes.

In the semi-arid climate which characterizes the basin area, vegetation is usually confined to stream banks and flood plains. This riparian vegetation provides a marked contrast to the non-vegetated interfluvial zones thus making stream identification easier than in a more uniformly vegetated region. Though many of the rivers, streams and tributaries occur on relatively flat plains, they show up on SAR imagery because of multiple radar reflections from the stream beds and associated vegetation having the effect of accentuating surface roughness (McCoy, 1967; Hall and Bryan, 1977). This is the case even though water in the channels gives no return.

Four orders of streams can be identified on the basin floor and on mountain slopes from the 1:450,000 scale Seasat image (Figure 2). More drainage information is discernable on mountain slopes which are in the look direction of the Seasat and X-Band radars because more energy is directly reflected back to the sensor. Typically four orders of streams can be identified on the X-Band imagery (Figures 3A and B) although greater detail can be discerned in some well-dissected regions within the VV polarized data. For comparison it should be pointed out that four stream orders can also be mapped using Landsat RBV imagery and USGS 1:250,000 scale topographic maps of the same area. On the 10 m resolution U2 imagery as many as 6 stream orders can be identified in some areas and gullies and ditches can be easily located. A direct comparison between the X-Band SAR and the Seasat SAR at the same scale was not accomplished in the study because when the Seasat image was photographically enlarged to the same scale as the X-Band image a loss of image quality and detail resulted.

Due to the high spatial resolution of the X-Band radar (15 m) and the roughness criterion of 1.1 cm, canals and drainage diversions in the area to the south of Willow Lake and Fremont Lake can be discerned (Figure 3A area "A"). Even though some of these canals and diversions are narrower than 15 m, the linearity of these features provides sufficient definition or contrast to allow their detection. Several lakes are present in the X- and L-Band radar scenes (Figure 3 area "B" and Figure 2 area "E"). Localized high returns in portions of the lakes can be seen on both of the images. The

bright returns are caused by different factors in each case because the images were acquired during different seasons. On the Seasat SAR image which was acquired during the summer, much of New Fork Lakes acts as a specular reflector and appears dark on the Seasat image. Other portions of New Fork Lakes give high returns due to ripples produced by wind action. This was inferred after analyzing meteorological data from surface weather maps at the time of the Seasat overpass which indicated wind speeds of about 5 m/s. Other lakes also give localized high returns as seen in Figure 2 (Fremont and Willow Lakes). Ripples on the lake surfaces are rough at the Seasat SAR wavelength and cause high reflections. The bright returns may be partially attributed to the steep (~70°) depression angle of the Seasat SAR. The darker, low return edges of New Fork Lakes may have been protected from the wind during the satellite overpass and thus are not rough at the Seasat SAR wavelength.

A portion of the Seasat SAR scene was enlarged using the digital data on the Atmospheric and Oceanographic Interactive Processing System (AOIPS) at Goddard Space Flight Center. This was done in order to determine how much additional detail could be obtained by doing a 1:1 sampling of the lines comprising the SAR data. The resulting subscene was enhanced by contrast stretching the spectral limits of the data in the subscene, and assigning new spectral limits. The image product, shown in Figure 6, does not show any additional detail, but allows one to enhance features of interest for better comparison with other imagery and topographic maps.

At the time in which the X-Band image was acquired (March 30, 1978) the lakes were completely ice-covered as determined through analysis of Landsat imagery. Localized bright returns within the lakes are particularly evident in the like polarized, VV, image as seen in Figure 3A, while the VH cross polarized imagery (3B) renders dark returns within the lakes. The localized bright returns are due to reflections from a rough ice surface and the snow/ice and ice/water interfaces and possibly air bubbles and cracks in the near surface ice as discussed by Page et al. (1975).

Snow was on the ground when the X-Band image was acquired in March. In the mountain area, above the lakes, the snow depth varied from 1.0 - 3.0 meters. In the basin, below the lakes, the snow was 0.5 - 1.0 meters thick (USDA, 1979). Radar penetrates the snow and detects the ground surface beneath the snowcover at the X- and L-Band wavelengths (Waite and MacDonald, 1970). In the

forested mountains, the tree canopy effectively camouflages the ground below because it reflects the microwaves before they can reach the snowcovered ground.

Glaciers and permanent snow fields are present in the highest elevations of the Wind River Mountains (Figure 1B). However these features cannot be discerned on the Seasat SAR image even though mountain or valley type glaciers have been seen on other L-Band SAR imagery largely as a result of their morainal patterns. Also valley glaciers are often heavily crevassed and represent a rough surface to the radar wavelength. In the Seasat SAR scene, Figure 2, the glaciers cannot be discerned from the surrounding terrain possibly because of their similarity in roughness to the terrain and the fact that they are alligned in a NW-SE direction and are thus not in the optimal look direction to provide a signature response significantly different from that of the surrounding terrain.

On the Landsat RBV and U-2 images, contrary to radar images, snow and ice are often the most easily observable features. However even with the Landsat and U-2 sensors, glaciers cannot be readily distinguished except in the late summer when the seasonal snowpack has melted. Figure 5B is a snowcovered U-2 scene taken in March of 1976. Compare this figure with Figure 3 which was taken in March of 1979 at which time the ground was also snowcovered. In the snowcovered U-2 scene there is a lack of detail of surface features compared to the detail in the radar image. The snow effectively conceals the underlying surface on the U-2 scene, but is penetrated by the radar. The utility of synthetic aperture radar in mapping many surface features is not seasonally dependent as are sensors which operate in the visible and near-infrared portions of the electromagnetic spectrum.

Because of differences in scale, resolution and possibly spectral differences between the X-Band and Seasat SARs, several features that were difficult to distinguish on Seasat were readily observable on the X-Band radar. For example, a marsh area is present to the north of New Fork Lakes where the New Fork River enters the upper lake (Figure 3B area A). This marsh is characterized by relatively low vegetation such as rushes and willow shrubs. The resulting radar returns are transitional in roughness between a rough and a smooth surface. In the X-Band imagery, the marsh area is more easily seen in the cross polarized (Figure 3B) than in the like polarized imagery (Figure 3A) because

the whole near nadir region is saturated in the like polarized imagery. The marsh area is not shown on the U-2 image. The town of Pinedale (Figure 3B area B) can be identified just to the south of Fremont Lake on the X-Band imagery. The bright returns are caused by differences in length and shape of the linear arrays of buildings that produce numerous corner reflectors (Ford, 1979). The striations and streaks in the area below Willow Lake (Figure 3A area C) are thought to be cattle paths and jeep trails which result from the ranching activity in the area. In addition, at area C on Figure 3B, a clear-cut area of conifers can be recognized. The bright stripes are trees that have not yet been harvested and the dark stripes are areas where almost all of the trees have been removed. These areas are relatively smooth and thus appear dark since they have no forest canopy. Another clear-cut area which is less distinguishable can be found just to the east of New Fork Lakes. On the Landsat RBV image (Figure 4), which is about the same scale as the Seasat SAR, the town of Pinedale is difficult to differentiate from the surrounding terrain, however the clear-cut areas can be identified. On the U-2 image (Figure 5) both the town of Pinedale and the clear-cut area are easily observable.

V. CONCLUSIONS

Based on the analysis of the Seasat image acquired over west-central Wyoming on July 31, 1978, it appears that the Seasat SAR does have a capability for hydrologic mapping even though it was primarily designed for oceanographic applications. Both the L-Band (Seasat) and the X-Band (aircraft) SAR imagery were found to be useful for observing drainage detail. Streams have bright signatures on the SAR imagery because the riparian vegetation produces a rough surface and thus high radar returns. Lakes appear relatively bright on the Seasat image presumably in response to surface ripples and waves induced by wind action. When the wind is calm the lakes act as specular reflectors and appear smooth or dark on the imagery. On the X-Band image, which was taken when the lakes were completely frozen, the lakes also have a bright signature because the ice surface is rough probably as a result of fractures, rafting, and wind action during ice formation. SAR imagery did not reveal snow at either the 23.5 cm (L-Band) or 2.8 cm (X-Band) wavelengths. The radar penetrates through the dry snow to the underlying surface, and thus may be useful for analyzing the topography beneath

the snowcover. In forested areas the tree canopy intercepts the radar signal and prevents it from reaching the snow surface.

Comparing Seasat and X-Band aircraft SAR imagery to Landsat RBV imagery, U-2 photography, and topographic maps of the Wind River Range area, it seems that the SAR data do not seem to provide as much hydrologic information as do the other sensors in the visible and near-infrared portions of the spectrum. Although the drainage detail extracted from the radar imagery is similar to that which can be detected with the visible wavelengths, much more information regarding snow hydrology can currently be acquired from the visible wavelengths than from L-Band and X-Band SAR. Radar, however, is useful for analyzing hydrologic features beneath snowcover, and shorter wavelength radar data may provide more information concerning snowpack properties than longer wavelength data.

An important advantage of radar is its all-weather day/night remote sensing capability. The utility of radar for hydrologic studies is optimized during inclement weather, e.g., during a flood when conventional data cannot be acquired due to cloudcover or darkness. For future satellite missions designed for hydrologic studies, the multispectral approach using visible, near-infrared, infrared, passive and active microwave (radar) wavelengths is obviously the optimum approach as opposed to using a single wavelength or sensor. It remains to be seen, however, if there is a synergistic effect on the overall results that would fully support the additional cost and complexity in the technology and data processing.

ACKNOWLEDGEMENTS

Dick Fenner and Doug LaPoint of NASA/Johnson Space Flight Center, Houston, TX, provided the C-130 aircraft radar data and Frank Barath of the Jet Propulsion Laboratory, Pasadena, CA, provided the Seasat SAR data.

REFERENCES

Ford, J.P. 1979: Analysis of Seasat Orbital Radar Imagery for Geologic Mapping in the Appalachain Valley and Ridge Province, Tennessee Kentucky Virginia. *Proc. of the Radar Geol. Workshop*. Snowmass, CO.

Hall, D.K. and M. L. Bryan, 1977: Multispectral Remote Observations of Hydrologic Features on the North Slope of Alaska. *Proc. of the Amer. Soc. of Photogrammetry Fall Tech-Mtg.*, October 18-21, Little Rock, AR pp. 393-424.

Kovaly, J.J., 1978: *Synthetic Aperture Radar*. Artech House, Inc. Dedham, MA, 1978, pp.21-31.

MacDonald, H.C. and W.P. Waite, 1973: Imaging Radars Provide Terrain Texture and Roughness Parameters in Semi-arid Environments. *Modern Geol.* vol. 4, no. 2, 1973, pp. 145-158.

Matthews, R.E. (ed.), 1975: *Active Microwave Workshop Report*, NASA SP-376, Wash., D.C. pp. 60-67.

McCoy, R.M.: An Evaluation of Radar Imagery as a Tool for Drainage Basin Analysis, CRFS. TR-61-31. Center for Research in Engin. Science, Univ. of Kansas, Aug. 1967.

Page, D.F. and R.O. Ramsier, 1975: Application of Radar Techniques to Ice and Snow Studies. *Jour. Glac.* V. 15, pp. 171-191.

Peake, W.H. and T.L. Oliver, 1971: The Response of Terrestrial Surfaces at Microwave Frequencies. Ohio State Univ. Electroscience Lab, Tech. Rep. AFAL-TR-70-301.

Sabins, F.F., R. Blom and C. Elachi, 1979: Expression of San Andreas Fault on Seasat Radar Image. *Proc. of the Radar Geol. Workshop*, Snowmass, CO.

Simonett, D.S., 1978: *Active Microwave Applications Research and Development Plan*. Santa Barbara Remote Sensing Unit Technical Report 2.

U.S. Dept. of Agriculture, 1979: *Soil Conservation Service: Water Supply Outlook for Wyoming as of April 1, 1979.*

Waite, W.P. and H.C. MacDonald: Snowfield Mapping with K-Band Radar. Remote Sensing of the Environment, vol. 1, no. 2, March 1970, pp. 143-150.

FIGURES

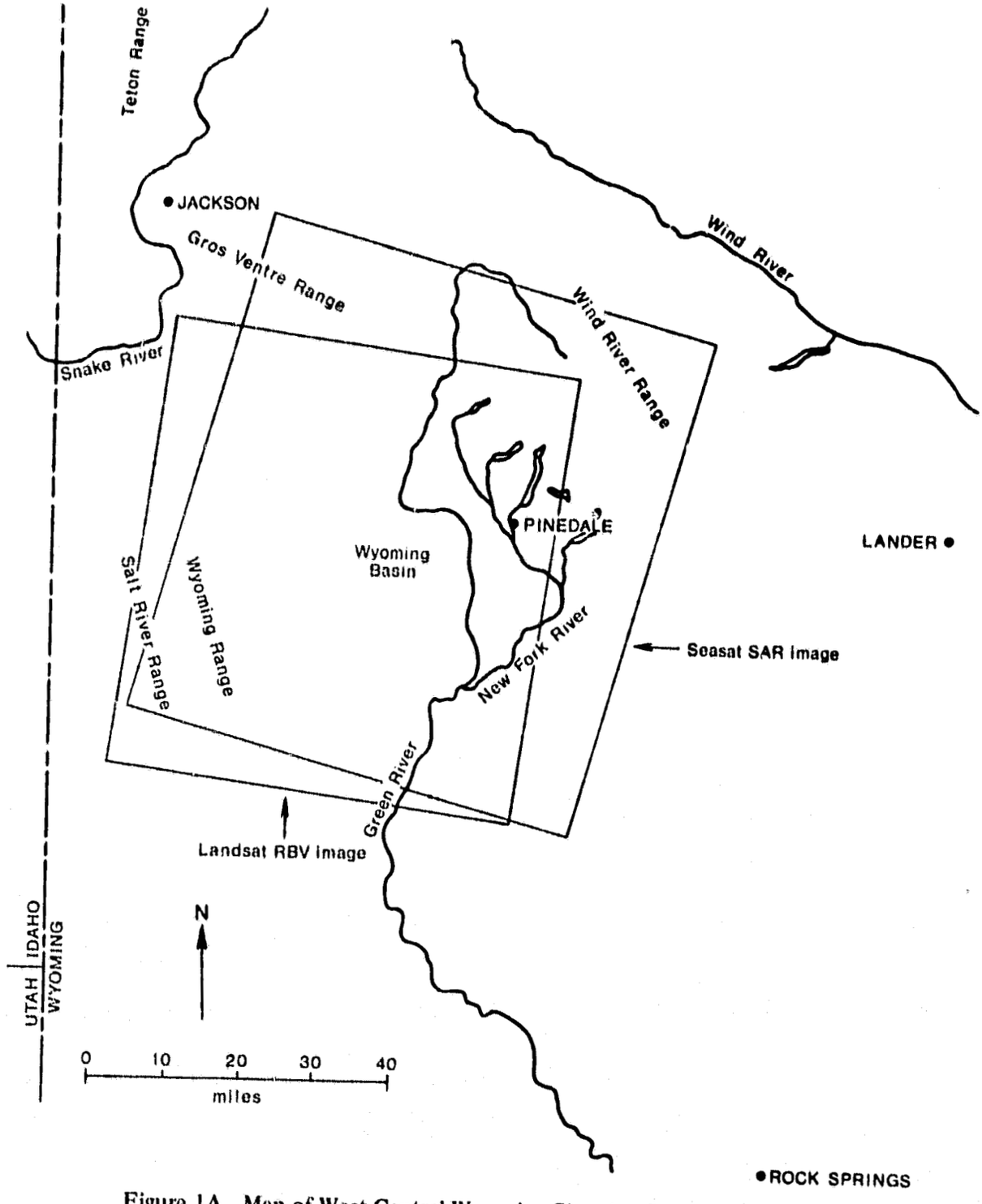

Figure 1A. Map of West-Central Wyoming Showing Seasat SAR and Landsat RBV Image Coverage

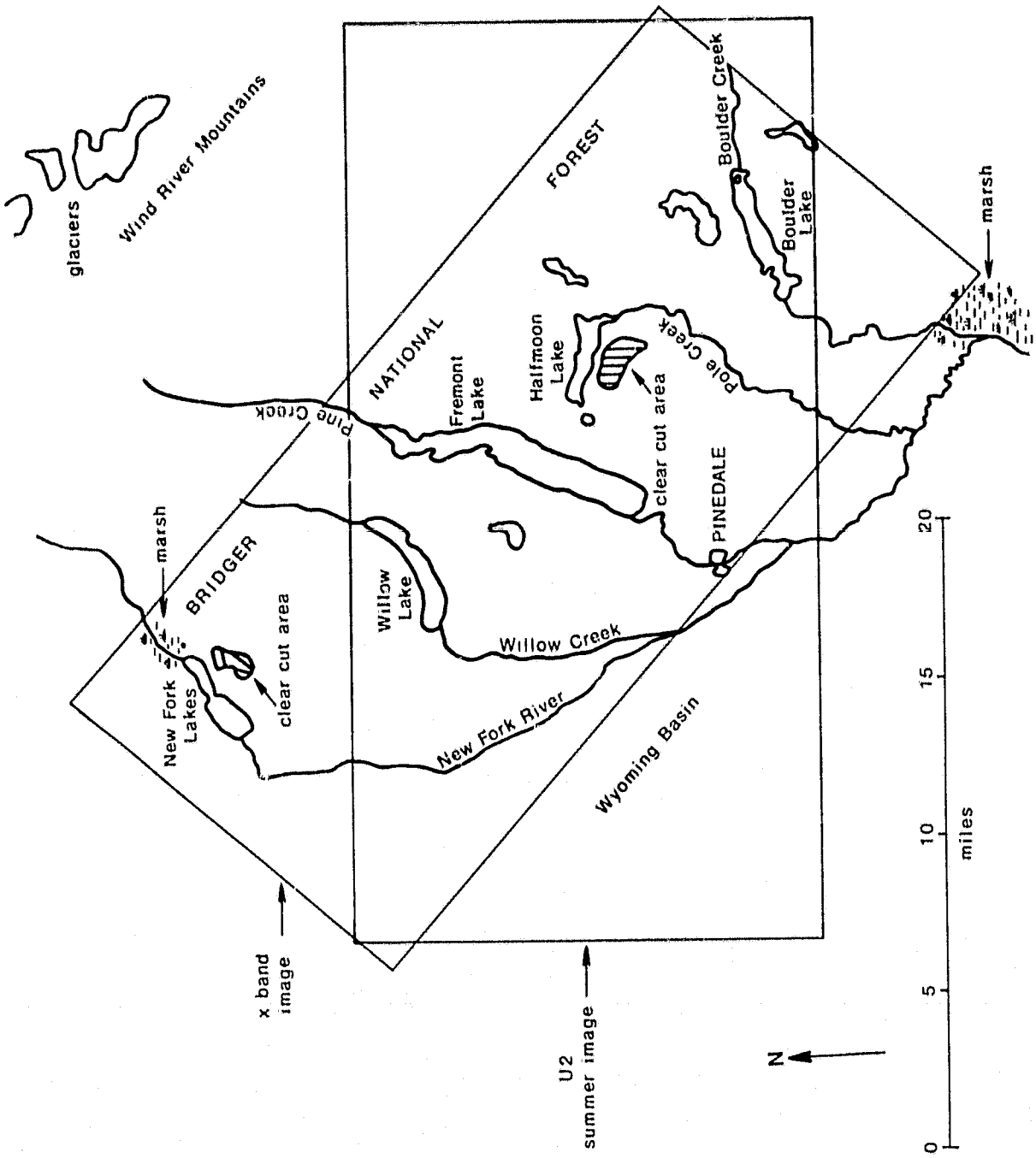

Figure 1B. Detailed Map of Portion of Figure 1A Showing X-Band and U-2 Image Coverage

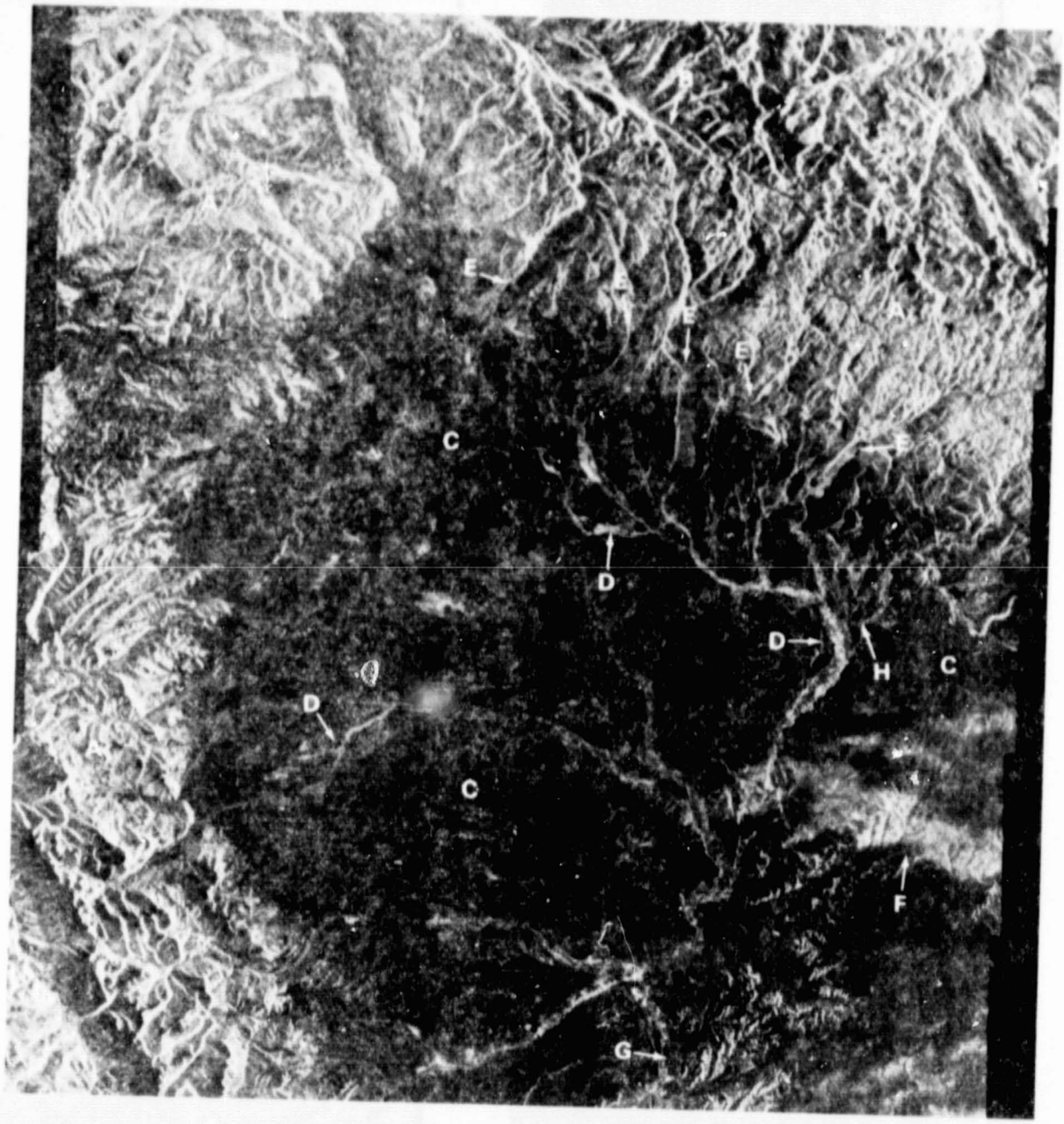

Figure 2. Seasat SAR Scene of West-Central Wyoming Taken on July 31, 1978. Look Direction Is Towards The Northwest.

Figure 3A. X-Baud SAR (VV) Damage Taken March 30, 1978

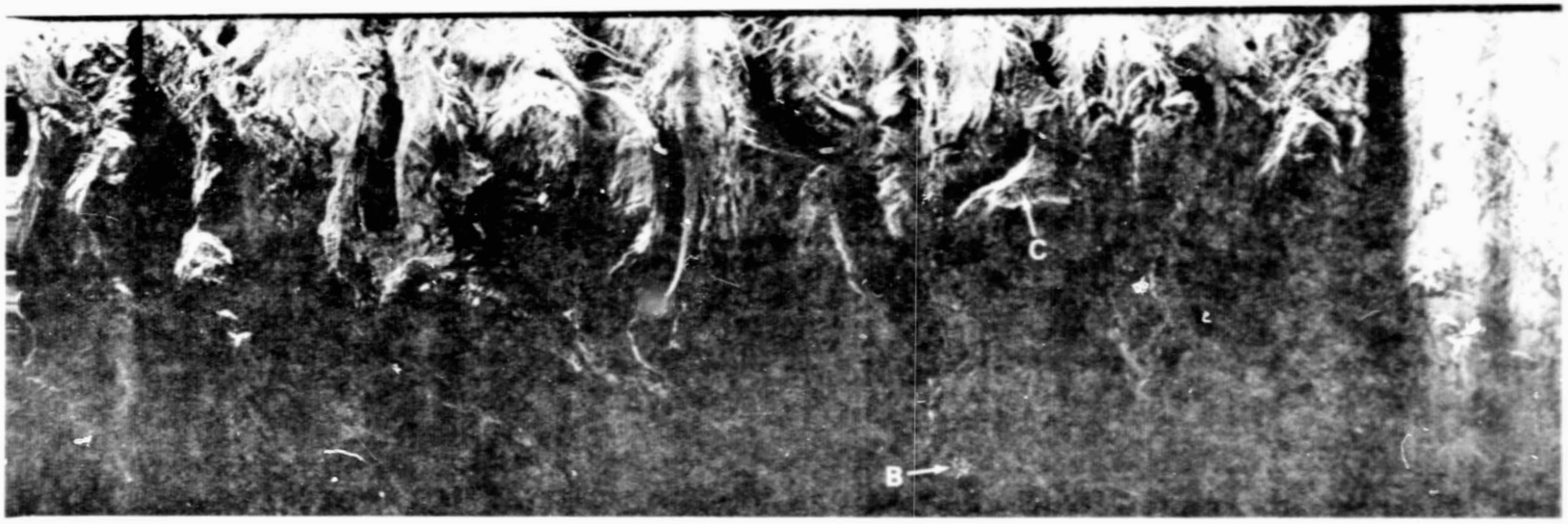

Figure 3B. X-Band SAR (VH) Image Taken March 30, 1978

11AUG78 C N42-53/W110-21 D040-030 N N43-02/W109-44 R C XROD SUN EL52 AI20 S2S- P-N L2 NASA LANDSAT E-30159-17245-C

Figure 4. Landsat RBV Image Taken August 11, 1978

Figure 5A. U-2 Summer Scene Taken June 1976

Figure 5B. U-2 Winter Scene Taken March 1976

Figure 6. Seasat SAR Enlargement of New Fork Lakes Subscene